Electronic topological and structural transition in $AuIn_2$ under pressure

B. K. Godwal
High Pressure Physics Division, Bhabha Atomic Research Centre, Mumbai, 400 085, India

A. Jayaraman
Hawaii Institute of Geophysics, 2525 Correa Road, Honolulu, Hawaii 96822

S. Meenakshi, R. S. Rao, S. K. Sikka, and V. Vijayakumar
High Pressure Physics Division, Bhabha Atomic Research Centre, Mumbai, 400 085, India

(Received 18 February 1997)

Electrical resistivity, thermoelectric power, and high-pressure x-ray-diffraction measurements are carried out to investigate the anomaly observed earlier in fusion data around 3 GPa in the intermetallic compound $AuIn_2$. While the imaging plate high-pressure angle-dispersive data indicate a structural phase transition beyond 8 GPa, the thermoelectric power shows a peak around 2 GPa, indicating the occurrence of an electronically driven isostructural transition. The first-principles linearized muffin-tin orbital calculations reveal that this transition is brought about by interception of the Fermi level by the energy-band maximum. The Lifshitz nature of this transition is responsible for the anomaly in the high-pressure electrical and fusion data. [S0163-1829(98)03502-4]

I. INTRODUCTION

Most of the materials that have fluorite, i.e., the calcium fluoride (CaF_2) (or anti-CaF_2), structure (space group $Fm3m$) are halides, oxides, or chalcogenides of univalent or tetravalent cations and show predominantly ionic bonding. However, a few intermetallics also crystallize in this structure.[1] In fact, gold forms intermetallic compounds of stoichiometry AB_2, with Al, Ga, and In (as B elements) in the CaF_2 structure. These compounds are known to exhibit low residual resistivities. The bright mauve color of $AuAl_2$, as opposed to the bluish shade of $AuIn_2$ and the neutral appearance of $AuGa_2$, is consistent with the observed differences in their optical transitions and band structure.[2] The other observed differences concern the anomalous Knight shift of Ga in $AuGa_2$ compared to the normal behaviour of Al and In in the other two compounds[3] and the different thermoelectric behavior of $AuGa_2$.[4] Also, the measurements of the electronic specific heat[5] and Hall coefficient[4] do not reveal any significant differences in these compounds. It is thus necessary to have detailed knowledge of the band structure for these compounds.

Storm, Wernick, and Jayaraman[6] studied the fusion behavior of these compounds up to a pressure of 5 GPa. Their measurements show that the fusion curve of $AuGa_2$ and $AuAl_2$ decreases with pressure, while that of $AuIn_2$ remains constant with almost zero slope to about 3 GPa and then acquires a positive slope with a further increase in pressure. Though this kind of behavior indicates the occurrence of a pressure-induced phase change in solid $AuIn_2$, no phase boundary was detected below the melting temperature and pressures up to 5 GPa. Thus the origin of this fusion anomaly is not clear and it is expected that high-pressure studies will help to unravel the cause of it.

As many oxides of geophysical interest occur in CaF_2 structure, phase transformation studies on intermetallic compounds under compression are useful to give indications of the high-pressure metallic phases of these oxides. Motivated by these factors, we have initiated a program to study these intermetallics for their high-pressure behavior. As a starting step, we have carried out angle-dispersive x-ray-diffraction (ADXRD), electrical resistivity, and thermoelectric power (TEP) measurements on $AuIn_2$ under pressure. As the electronic structure is very sensitive to pressure, the electronic band structure in the CaF_2 structure under compression was also computed to substantiate the interpretations of experimental findings, and to the best of our knowledge only nonrelativistic, non-self-consistent, or parameter-based calculations at ambient pressure exist[7] in the literature. The relevant de Haas–van Alfen studies on $AuAl_2$, $AuGa_2$, and $AuIn_2$ also exist,[2] and though these experiments conclusively identify many of the orbits in $AuAl_2$, only a few could be properly identified in the other two systems.

II. EXPERIMENTAL DETAILS

The details of the manner in which the $AuIn_2$ sample was prepared has been discussed by Storm *et al.*[6] For electrical resistivity and TEP measurements, initially pellets of the samples of approximate size $2\times3\times5\ mm^3$ were prepared and then pressed between tungsten carbide (WC) anvils to a load of 5 tons. The well-compacted material was then trimmed to 1.5-mm-long and 2.5-mm-wide pieces and used for the high-pressure electrical and TEP measurements. An opposed Bridgeman anvil setup,[8] consisting of 12-mm-face-diameter WC anvil pairs, two 0.15-mm-thick pyrophylite gaskets, and talc pressure medium, with *in situ* Bi pressure calibration, was employed. Resistance was measured by the four-probe technique. For TEP measurements, Chromel and Alumel thermocouple wires were employed.[8,9] A thin Mylar sheet between the talc and electrical leads ensured clean electrical contact with the sample.

Zr-filtered x rays from a rotating anode generator with Mo target and an imaging plate area detector[10,11] were employed in the ADXRD measurements. The $AuIn_2$ powder along with a ruby chip as pressure marker and with ethanol-methanol as pressure medium was loaded in a Bassett-type diamond anvil cell (DAC).[12] The diffracted x rays from the sample were recorded on a 25×20 cm molecular dynamics imaging plate[11] (IP) placed behind the DAC. The recorded data on the IP were read out in two dimensions (2D). The scanning step (pixel size) was 88 μm and the intensity digitized to 16 bits. The readout data were displayed on a computer monitor for a quick check of the data quality and for a preliminary analysis. In order to transform the digitized image into a standard one dimensional (1D) powder pattern expressed in terms of 2θ, the sample-to-IP distance was accurately determined (7.62 cm) from the diffraction pattern of gold at ambient conditions. The diffraction profile was obtained by integrating the intensity along the azimuthal direction at each radial step. This yielded precise determination of lattice constants at different pressures.

III. DETAILS OF CALCULATIONS

In order to confirm the experimental interpretations and for further understanding of the behavior of $AuIn_2$ around the 3-GPa pressure region, we carried out the first-principles electronic structure calculations by the linearized muffin-tin orbital[13] (LMTO) method in the CaF_2 structure for various compressions. To make the structure close packed, one empty sphere (of radius equal to that of a Au atom) was inserted at the center of the fcc primitive cell (0.5, 0.5, 0.5), with the Au atom at the corners (0,0,0) and In atoms at (0.25, 0.25, 0.25) and (0.75, 0.75, 0.75). An In-to-Au radii ratio of 1.08 was used. The atomic sphere approximation[13] (ASA), the local density approximation[14] (LDA), and frozen core were employed in the LMTO method. With the introduction of empty spheres, the maximum overlap among the atomic spheres was 24.8%. We also included the combined correction terms[13] and the muffin-tin corrections[15] to the electrostatic Coulomb interaction in the total energy. The valence configurations for Au and In were taken as $6s^15d^{10}$ and $5s^25p^1$, respectively. The s, p, d, and f components of the angular momentum expansion of the orbitals were retained. We calculated the total energies by considering the relativistic spin-orbit effects through perturbation. The Slater exchange[16] reduced by a factor of 0.8 gave the minimum of the total energy curve at the experimentally known volume for the ambient pressure, and this exchange formula was used at all compressions. Calculations were carried out for 95 **k** points in the irreducible wedge of the Brillouin zone.

IV. RESULTS AND DISCUSSION

The electrical resistivity decreases with pressure, and the slope of its variation changes rapidly near 2 GPa (Fig. 1). The TEP also shows a deviation from a monotonous increase in the 2–4 GPa pressure range with a peak near 2 GPa (Fig. 2). These indicate the possibility of electronic or structural changes in this pressure region.

To obtain the equation of state (EOS), we calculated the pressure[17] at each volume from the contributions arising from the conduction electrons evaluated by the LMTO-ASA method, along with the correction for intercellular Coulomb interaction beyond the ASA.[15,18] In order to compare it with the EOS determined from the high-pressure ADXRD technique, we included the thermal pressure at room temperature and the pressure arising from zero-point vibrations.[17,19] In Fig. 3 we have compared the theoretically calculated EOS with measured high-pressure data.[20] Our experimental data yielded the isothermal bulk modulus (K_0) of 50 GPa using 4 as the value of K_0' (the pressure derivative of K_0). The computed EOS is much harder than the measured one. Discrepancies of this nature are not unusual in first-principles electronic structure calculations. The quantitative agreement can be improved[21] by applying the generalized gradient approximation[22] for exchange correlation terms and/or by using the full potential LMTO method. However, these improvements are not expected to change drastically the main conclusions of the present work. The P-V data of Fig. 3 do not reveal any discontinuity in volume around 3 GPa, and it continues to remain smooth up to 8 GPa. For a more detailed analysis, we studied the universal EOS from theoretical P-V estimates. The universal EOS, as given by Rose *et al.*,[23] is as follows:

$$\ln H=\ln[PX^2/3(1-X)]=\ln K_0+\eta(1-X),$$

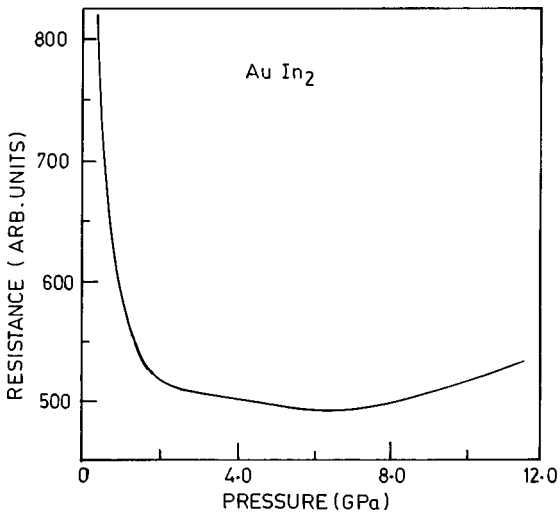

FIG. 1. Variation of resistance with pressure at room temperature in $AuIn_2$.

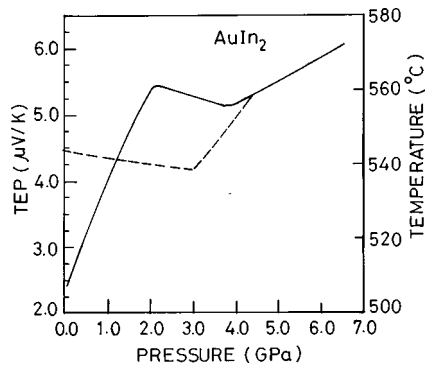

FIG. 2. Thermoelectric power as a function of pressure at room temperature in $AuIn_2$. The fusion curve from Ref. 6 is also shown for comparison.

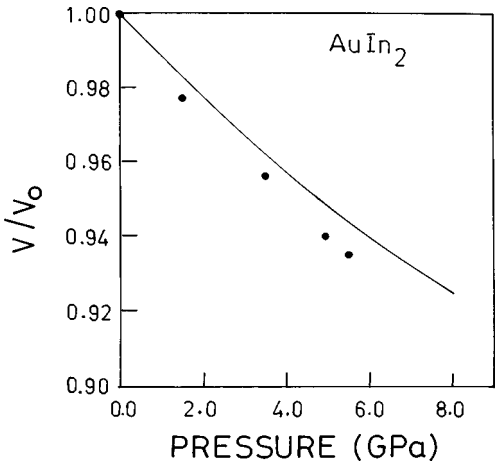

FIG. 3. V/V_0 vs pressure for $AuIn_2$. The solid line is from calculations, while the dashed line from ADXRD measurements.

where $X=(V/V_0)^{1/3}$, P is the pressure, V_0 the normal volume, and η is related to K_0' by

$$\eta=3(K_0'-1)/2.$$

In Fig. 4, we display the universal EOS [i.e, ln H versus $(1-X)$] which is seen to deviate from linearity in the 2–4 GPa pressure range where the electronic transitions take place. Thus the present observation based on universal EOS is consistent with the findings of Sikka.[24]

On increasing the pressure beyond 8 GPa, $AuIn_2$ transforms to another phase (Fig. 5) which is stable up to 15 GPa. On unloading, it back transforms to the CaF_2 phase only below 2 GPa. This structural transition results in an increase in resistivity at the transition (see Fig. 1). In Table I we give the measured d values at 9 GPa. As seen from the table, the high-pressure diffraction pattern can be indexed on a monoclinic cell (with space group $P2_1/c$ with $a=10.14$ Å, $b=4.19$ Å, $c=8.78$ Å, and $\beta=89°$). This distorted Co_2Si-type structure is the post-cotunnite phase[25] where the coordination of Au with In is 10. More structural details will be published separately.[26]

Although the electrical transport properties like resistivity and TEP and the computed universal EOS indicate the possibility of some significant electronic changes occurring in the 2–4 GPa range of pressure, the ADXRD measurements rule out the possibility of a structural change up to 8 GPa. Thus the isostructural electronic structure change appears to be responsible for the observed anomaly in resistivity, TEP, and fusion curve. The discrepancy between the anomalies in the fusion curve and the TEP data (see Fig. 2) can be attributed to temperature effects. It may be noted that in the fusion curve measurements, no other phase boundary was detected below the melting point up to 5 GPa. Thus the possibility that the change of slope in the fusion curve, being caused by the Co_2Si-CaF_2 phase boundary intersecting it, is ruled out.

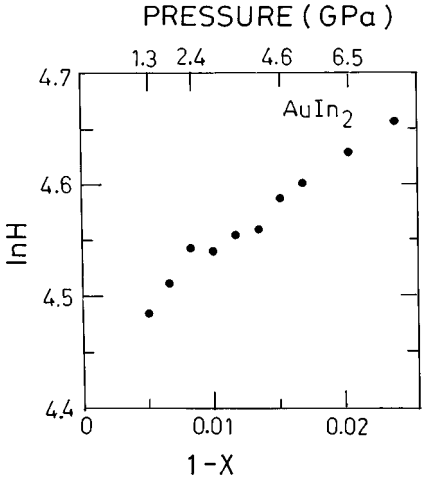

FIG. 4. Universal equation of state for $AuIn_2$. The pressure values of interest are also marked.

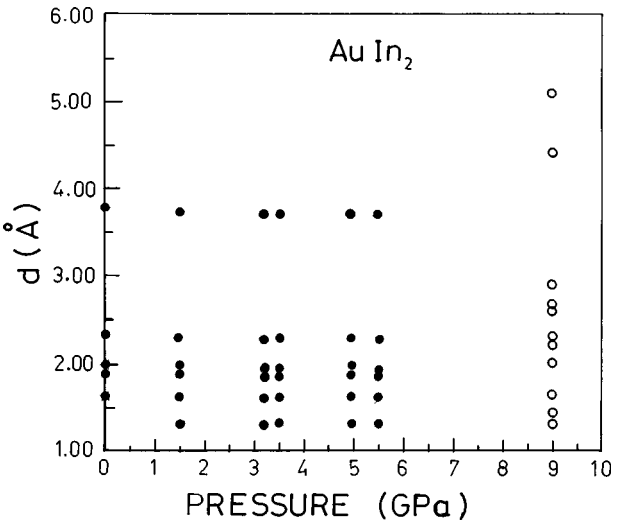

FIG. 5. Variation of the measured d spacings with pressure. The open circles denote the values for the high-pressure Co_2Si phase at 9 GPa.

A significant feature observed through the LMTO calculations is the crossing of the Fermi level (E_F) by an electron energy-band maximum at about 2.2 GPa pressure. As shown in Fig. 6, the X_3-$\Gamma_{2'}$-L_1 energy band, which is occupied at the ambient pressure, shifts upwards with respect to E_F and becomes flatter around the Γ point. Thus the indications from

TABLE I. Observed d values compared with the d values calculated using a monoclinic cell (space group $P2_1/c$). The two sets of hkl indices correspond to the two calculated d values.

$d_{observed}$	$d_{calculated}$ using a monoclinic cell ($a=10.14$ Å, $b=4.19$ Å, $c=8.78$ Å, $\beta=89°$)	hkl
5.071	5.072	2 0 0
4.399	4.390	0 0 2
2.870	2.894	1 1 −2
2.642	2.631	3 1 0
2.551	2.554	2 0 3
2.277	2.270	3 1 2
2.177	2.179	4 0 −2
1.980	1.983	5 0 1
1.617	1.619, 1.615	0 1 5, 4 2 0
1.395	1.393, 1.397	5 1 −4, 0 3 0
1.289	1.289	7 0 −3, 2 3 2

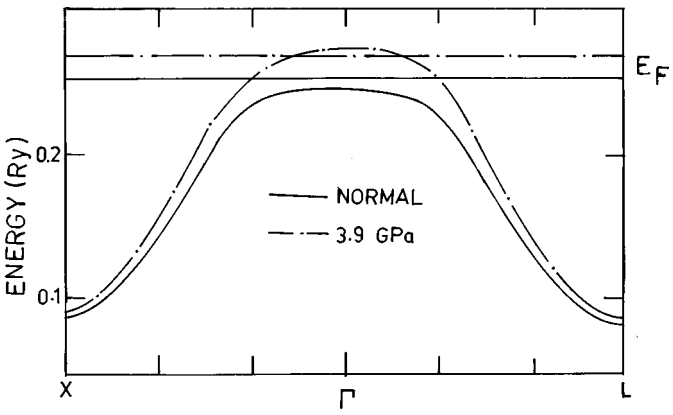

FIG. 6. Shift of the energy band maximum at $\Gamma_{2'}$ across the Fermi level, from the occupied to unoccupied region, under pressure.

the electronic-structure calculations are that the anomaly in resistivity and TEP should be due to a Lifshitz singularity[27] [also referred as an electronic topological transition (ETT)] when the extremum of an electron energy band passes through E_F. This effect is enhanced in $AuIn_2$ due to the flatness of the band near the Γ point. Lifshitz[27] has shown that close to the ETT, the electron free energy has a $|\Delta|^{5/2}$ term (where $\Delta = E_F - E_{\Gamma 2'}$), and causes anomalies in the thermodynamic and kinetic properties. In our electrical resistance data, this ETT results in a slower rate of decrease of resistance with pressure in the 2–6 GPa range. Thus we attribute the observed anomalies in electrical resistivity, TEP, and the fusion data under pressure to the ETT. However, the sharp decrease of the resistance below 2 GPa is unusual in metals. It is not due to contact resistance (see Sec. II). Our detailed calculations had shown that there is not much change in the density of states at E_F in this region of pressure.[28] Thus the present studies do not enable a comprehensive understanding of this rapid change below 2 GPa, and the study of the electron-phonon interaction with pressure may be useful.

To conclude, the 3-GPa anomaly observed in melting data of $AuIn_2$ is due to an isostructural transition with no observable volume discontinuity. The theoretical band-structure results reveal that this transition is brought about by the crossing of the Fermi level by the energy-band maximum from the occupied to the unoccupied level and is discernible in the universal EOS by its deviation from linearity around that pressure. This Lifshitz transition is also responsible for the observed anomaly in the high-pressure resistivity and TEP data.

[1] C. Barrett and T. B. Massalski, *Structure of Metals*, McGraw-Hill Series in Material Science and Engineering (Eurasia, New Delhi, 1966).
[2] J.-P. Jan, W. B. Pearson, Y. Saito, M. Springford, and I. M. Templton, Philos. Mag. **12**, 1271 (1965).
[3] V. Jaccarino, W. E. Blumberg, and J. H. Wernick, Bull. Am. Phys. Soc. **6**, 104 (1961).
[4] J.-P. Jan and W. B. Pearson, Philos. Mag. **8**, 279 (1963).
[5] J. A. Rayne, Phys. Lett. **7**, 114 (1963).
[6] A. R. Storm, J. H. Wernick, and A. Jayaraman, J. Phys. Chem. Solids **27**, 1227 (1966).
[7] A. C. Switendick and A. Narath, Phys. Rev. Lett. **22**, 1423 (1969); S. Kim, J. G. Nelson, and R. S. Williams, Phys. Rev. B **31**, 3460 (1985).
[8] V. Vijayakumar, B. K. Godwal, Y. K. Vohra, S. K. Sikka, and R. Chidambaram, J. Phys. F **14**, L65 (1984).
[9] A. K. Singh and G. Ramani, Rev. Sci. Instrum. **49**, 1324 (1978).
[10] The rotating anode x-ray generator is based on Rigaku Rotaflex (RTP 300 RC) model.
[11] The image plate system is based on a 425E molecular dynamics phosphor imager model; O. Shimomura and K. Takemura, Rev. Sci. Instrum. **63**, 967 (1992).
[12] A. Jayaraman, Rev. Mod. Phys. **55**, 65 (1983).
[13] O. K. Andersen, Phys. Rev. B **12**, 3060 (1975); H. L. Skriver, *The LMTO Method* (Springer, Berlin, 1984); N. E. Christensen, Phys. Rev. B **32**, 207 (1985).
[14] P. Hohenberg and W. Kohn, Phys. Rev. **136**, 864B (1964); W. Kohn and L. J. Sham, *ibid.* **140**, 1133A (1965).
[15] D. Glotzel and O. K. Andersen (unpublished); E. Esposito, A. E. Carlsson, D. D. Ling, M. Ehrenreich, and C. D. Gelatt, Jr., Philos. Mag. A **41**, 251 (1980); H. L. Skriver, Phys. Rev. B **31**, 1909 (1985); N. E. Christensen and S. Satpathy, Phys. Rev. Lett. **55**, 600 (1985).
[16] J. C. Slater, Phys. Rev. **81**, 385 (1951).
[17] B. K. Godwal and R. Jeanloz, Phys. Rev. B **41**, 7440 (1990).
[18] N. E. Christensen, Phys. Rev. B **32**, 207 (1985).
[19] S. Meenakshi, B. K. Godwal, R. S. Rao, and V. Vijayakumar, Phys. Rev. B **50**, 6559 (1994).
[20] Maximum error bars on the measured volumes are less than 3%.
[21] S. Meenakshi *et al.* (unpublished).
[22] J. P. Perdew, J. A. Chevary, S. H. Vosko, K. A. Jackson, M. R. Pederson, and D. J. Singh, Phys. Rev. B **46**, 6671 (1992); J. P. Perdew and Y. Wang, *ibid.* **45**, 13 244 (1992).
[23] J. H. Rose, J. R. Smith, F. Guinea, and J. Ferrante, Phys. Rev. B **29**, 2963 (1984).
[24] S. K. Sikka, Phys. Rev. B **38**, 8463 (1988).
[25] J. M. Leger, J. Haines, and A. Atouf, Phys. Rev. B **51**, 3902 (1995).
[26] V. Vijayakumar *et al.* (unpublished).
[27] I. M. Lifshitz, Sov. Phys. JETP **11**, 1130 (1960); L. Dagens, J. Phys. F **8**, 2093 (1978).
[28] B. K. Godwal, in *Advances in High Pressure Science & Technology*, edited by A. K. Singh (Tata McGraw-Hill, New Delhi, 1995), p. 23.